Local Structure in Spider Dragline Silk Investigated by Two-Dimensional Spin-Diffusion Nuclear Magnetic Resonance†

J. Kümmerlen,‡,§ J. D. van Beek,‡ F. Vollrath,⊥ and B. H. Meier*,‡

NSR-Center for Molecular Structure, Design and Synthesis, Laboratory of Physical Chemistry, University of Nijmegen, Toernooiveld, 6525 ED Nijmegen, The Netherlands, and Department of Zoology, University of Aarhus, Universitetsparken B135, DK 8000 Aarhus C, Denmark

Received July 27, 1995; Revised Manuscript Received January 28, 1996⊗

ABSTRACT: The local structure of dragline silk from the spider *Nephila madagascariensis* is investigated by solid-state nuclear magnetic resonance. Two-dimensional (2D) spin-diffusion experiments show that the alanine-rich domains of the protein form β-sheet structures in agreement with one-dimensional NMR results from a different species of the genus *Nephila* (Simons, A.; Ray, E.; Jelinski, L. W. *Macromolecules* **1994**, *27*, 5235) but at variance with diffraction results. The microstructure of the glycine-rich domains is found to be ordered. The simplest model that explains the experimental findings is a 3_1-helical structure. Random coils, planar β-sheets, and α-helical conformations are not found in significant amounts in the glycine-rich domains. This observation may help to explain the extraordinary mechanical properties of this silk, because 3_1-helices can form interhelix hydrogen bonds.

(1) Introduction

Spider dragline silk is a remarkable biopolymer: its mechanical properties are a unique combination of high tensile strength and high elasticity.[1−4] In contrast to the synthesis of man-made high-performance materials (e.g. steel or Kevlar) spider silk is synthesized at ambient temperature and pressure. The polypeptides that form the spider's dragline are produced in a set of glands (the major ampullate) and channeled through a duct to the spigot.[5,6] It seems that the solvent (water) is extracted in the duct, and that the silk goes into a liquid crystalline phase.[7,8] At the end of the duct the silk is drawn through a valve where it apparently forms the fiber, now insoluble in all but the most aggressive solvents; remaining free water evaporates quickly in the air.[9] The extraordinary properties of the spider's dragline silk make it attractive to think about technically produced analogues with well-defined amino-acid sequences (see ref 10 and references therein). To do so, it is essential to understand the macroscopic properties of dragline silk in terms of its microscopic structure including the amino-acid sequence of the protein (the primary structure), the (local) folding of the strands (its secondary structure), the packing arrangement (crystalline or amorphous regions) in the solid fiber, and possible superstructures. The observations that water can act as a plasticizer for some of the silks produced by spiders[11−13] and that wetting of the dragline silk can lead to a phenomenon called supercontraction[9] are a clear indication that the knowledge of the amino-acid sequence alone is not sufficient to understand the properties of silk but that detailed knowledge of the secondary structure, the packing, and the interplay with resident and ambient water is required.

Solid-state NMR can probe the local structure in disordered systems where the lack of translational long-range order makes the application of diffraction technique difficult.[14] The most useful NMR interaction for structural studies is the magnetic dipole interaction because of its simple and quantitative relationship to the atomistic structure of the material. In the simplest case, e.g. for an isolated spin pair, the dipolar interaction manifests itself as a line splitting from which the internuclear distance can directly be evaluated. If the spectral resolution is insufficient, the investigation of the dynamics of the dipolar-induced polarization transfer between the nuclei can be used to determine the distance.[15−17] For samples with a regular or random distribution of many coupled spins the spatial transfer of polarization, often called spin diffusion,[18] is the most useful source of geometrical information on the local structure.[17,19−28] Combined with two-dimensional (2D) NMR spectroscopy[29,30] it can be used to determine the relative orientation of neighboring molecular segments in crystalline and amorphous materials.[22−26,28,31,32] The resulting 2D spin-diffusion correlation maps directly relate to the local geometry if the purely spectral contributions are corrected for, or eliminated by, suitable pulse schemes.[17,28,33] Here we apply these methods that use two-particle NMR interactions to dragline silk. Solid-state NMR methods that employ one particle interactions, in particular the chemical shift, have already been applied to dragline silk. In a recent study, Simmons *et al.*[34] have used the empirical dependence of the isotropic chemical shift of the C_α and C_β resonances on conformation[35] to obtain information about the secondary structure of alanine in the dragline.

The spider silk most investigated is the dragline forcibly silked from the neotropical golden silk spider *Nephila clavipes*. The molecular weight of dragline silk was determined to be on the order of 200−350 kDa.[36,37] The primary structure of the major ampullate gland protein (dragline) is still not known completely. The results of Lewis[38] suggest that *N. clavipes* dragline silk is composed from two different proteins designated as spidroin I and spidroin II. In an independent study Mello *et al.*[37] have confirmed the existence of spidroin I. The primary structure of spidroin I contains $(Gly-Gly-X)_m$ segments (where X = Gln, Ala, Tyr, Ser, or Leu and $m = 3-6$ if minor sequence errors are tolerated) and Ala_n segments (with $n = 4-7$). In a simplified view, silk may be looked at as a block copolymer with glycine-

† Presented in part at the 36th Experimental NMR conference, April 1995, Boston, MA.

‡ University of Nijmegen.

§ Present address: Bayerisches Geo-Institut, Universtät Bayreuth, 95440 Bayreuth, Germany.

⊥ University of Aarhus.

⊗ Abstract published in *Advance ACS Abstracts,* March 15, 1996.

0024-9297/96/2229-2920$12.00/0

rich and alanine-rich domains. Diffraction results[39,40] clearly indicate that dragline silk is a heterogeneous material with "amorphous" and "crystalline" domains. It is generally accepted that the "crystalline" domains consist of protein segments that adopt an ordered β-sheet conformation. Controversy has, however, arisen whether these β-sheets are formed by the alanine-rich[34,38] or the glycine-rich[40,41] segments of the protein. The structure of the "amorphous" domains is largely unknown. It was suggested[3,6,41] that they are formed from irregularly packed α-helical protein segments or random coils, while other authors[34] find no evidence for such structures.

In this report we present an investigation of dragline silk that uses the magnetic dipolar interaction. The silk was collected from the species *Nephila madagascariensis* whose relatively large body size facilitates the collection of comparatively large samples. Local ordering is found and interpreted for both the alanine- and glycine-rich domains of the protein.

(2) Materials and Methods

Silk was reeled from *N. madagascariensis* in the standard way[42] at a speed of 26 cm/min. The spiders were kept at a low diet (of Tenebrio mealworms) supplemented with daily doses (starting a week before silking) of either [1-^{13}C]alanine or [1-^{13}C]glycine in an aqueous solution. The isotopic enrichment of the amino acids exceeded 98%, and in the resulting silk 60% enrichment was found.

NMR spectra were obtained on Bruker MSL 300, MSL 400, and AM 500 spectrometers. Approximately 45 mg of sample was used. Radio-frequency field strengths of typically 50 kHz have been used on carbon and proton channels. Cross-polarization contact times of 2 ms were used unless specified differently in the text; the recycle delay between scans was set to 4 s.

The 2D ^{13}C proton-driven polarization-transfer experiments[17,30] were recorded on static samples using the pulse sequence CP$-t_1-\pi/2-\tau_m-\pi/2-t_2$ with proton decoupling and quadrature detection in both dimensions. During the mixing time, no rf was applied.[17] For some experiments, a one-dimensional version of the spin-diffusion experiment, CP-TOSS$-\pi/2-\tau_m-\pi/2-t_2$, as suggested by Yang *et al.*,[43] was used; mixing times τ_m have been set to be equal to a multiple of a rotor period by means of an external synchronization apparatus.[44,45]

The solid-state NMR data will be interpreted by assuming that no significant transfer of the ^{13}C label to other amino acids takes place by the metabolism of the spider. The solid-state spectra of silk containing $^{13}C_1$-labeled alanine and $^{13}C_1$-labeled glycine, presented below, make it immediately evident that no significant amounts of ^{13}C are transferred to any aliphatic carbon position because no enhancement of any of these resonances is found. Because the carboxylic resonances from different amino acids are not resolved in the solid-state spectra, additional experiments were performed to investigate if any significant amounts of ^{13}C label are transferred between the carboxylic positions of different amino acids. For that purpose, silk containing doubly ^{13}C-labeled glycine was produced. The proton-decoupled ^{13}C liquid-state NMR spectra of a hydrolyzed sample of this silk (in 6 N HCl) were found to still contain the characteristic doublets caused by the ^{13}C—^{13}C J coupling between directly bound C=O and C_α ^{13}C. The center frequencies corresponded to a chemical shift of 171.4 and 42.1 ppm, respectively, identifying glycine. The resonances of other amino acids did not show significant enhancement. As expected, the strongest signal for nonlabeled amino acids was found for alanine (resonances at 174.8, 51.2, and 17.8 ppm). The C=O and C_α resonances of alanine showed, however, a doublet contribution indicative of some transfer of glycine to alanine by the spider's metabolism. The amount of label metabolized was approximately 5% and can be neglected for the interpretation of our solid-state spectra.

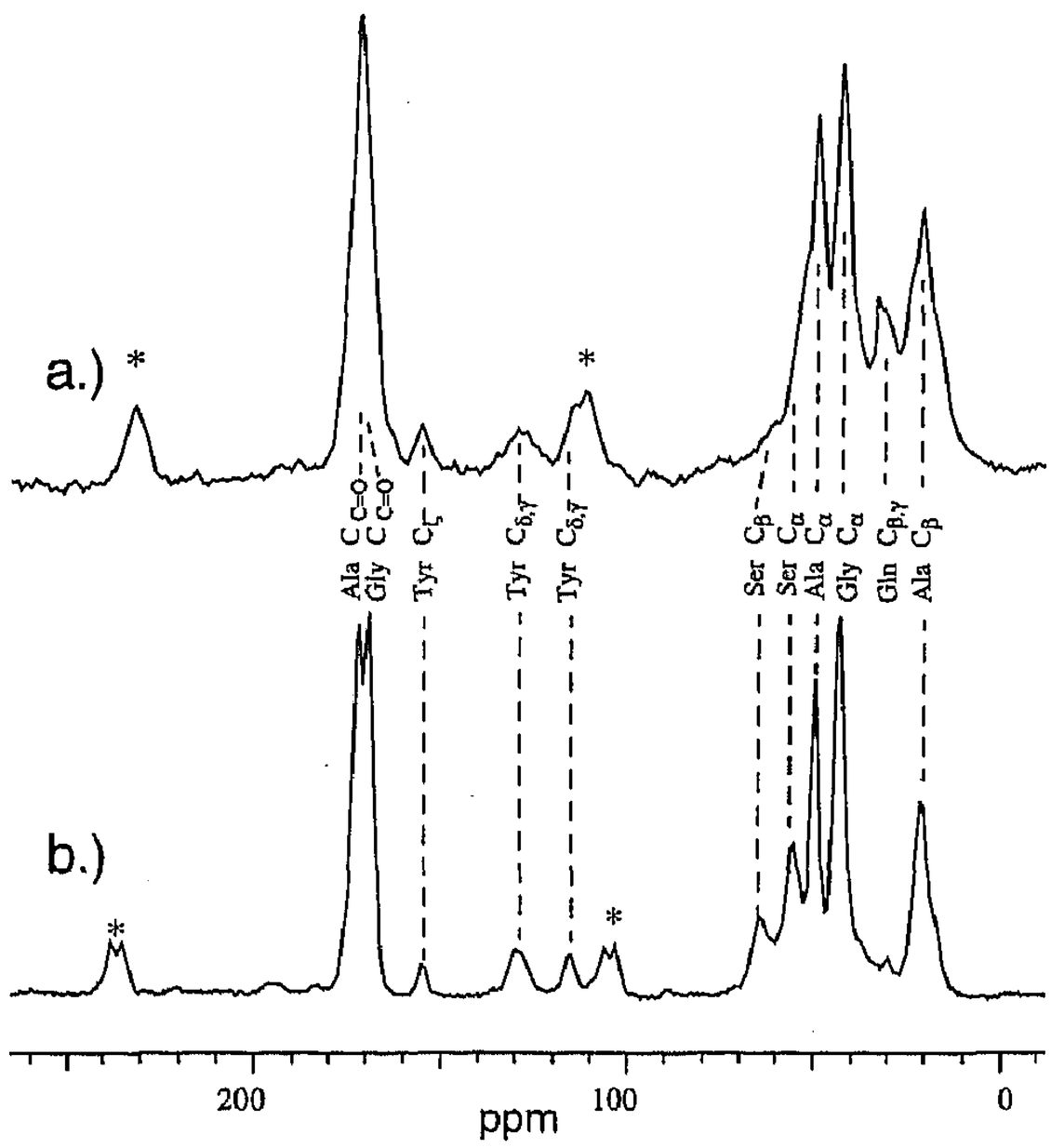

Figure 1. (a) 1D ^{13}C CP/MAS spectrum of *N. madagascariensis* dragline silk at a carbon resonance frequency of 100.63 MHz. A spinning frequency of 5.9 kHz was used. A total of 11 480 transients were acquired. (b) 1D ^{13}C CP/MAS spectrum of *B. mori* silk at 100.63 MHz resonance frequency at a spinning frequency of 6.8 kHz. A total of 5760 transients were coadded. Spinning sidebands are denoted by asterisks.

Table 1. Chemical Shift Parameters for Carbons in *N. madagascariensis* Dragline Silk[a]

carbon	δ_{iso}	δ_A	η
Gly C_α	43.3		
Gly C=O	169.7	-112.8 ± 2	0.87 ± 0.06
	172.5	-112.7 ± 2	0.87 ± 0.06
Ala C_β	20.2		
Ala C_α	48.9		
Ala C=O	172.5	-110.5 ± 2	0.82 ± 0.06
Gln $C_{\beta,\gamma}$	31.9		
Ser C_α	53.8		
Ser C_β	63.0		

[a] Tensor parameters are given according to Häberlen's notation[66] with $\delta_{iso} = (\delta_{11} + \delta_{22} + \delta_{33})/3$; $|\delta_{33} - \delta_{iso}| \geq |\delta_{11} - \delta_{iso}| \geq |\delta_{22} - \delta_{iso}|$; $\delta_A = 3(\delta_{33} - \delta_{iso})/2$.

(3) Results and Discussion

(3.1) One-Dimensional ^{13}C CP/MAS Spectra. The natural abundance ^{13}C CP/MAS spectrum of *N. madagascariensis* dragline silk is depicted in Figure 1 along with a tentative assignment of the individual resonances, obtained by comparison with the previously assigned spectrum from the silk produced by the silkworm *Bombyx mori*.[35] As expected, the spectrum of the dragline silk is similar to the one obtained by Simmons *et al.*[34] for dragline silk from *N. clavipes*. The aliphatic resonances of the three most abundant amino acids: glycine, alanine, and glutamine, are fairly well resolved. The C_α and C_β resonances of serine are partially hidden due to overlap with the C_α resonance of alanine. The carboxylic resonances of all amino acids overlap and lead to a single slightly asymmetric resonance at approximately 172.3 ppm. The observed isotropic chemical shifts are compiled in Table 1. To obtain the carboxylic chemical shifts of glycine and alanine and to get simplified spectra containing only carboxylic resonances, [1-^{13}C]alanine (Ala)- and [1-^{13}C]-glycine (Gly)-labeled samples were prepared. This

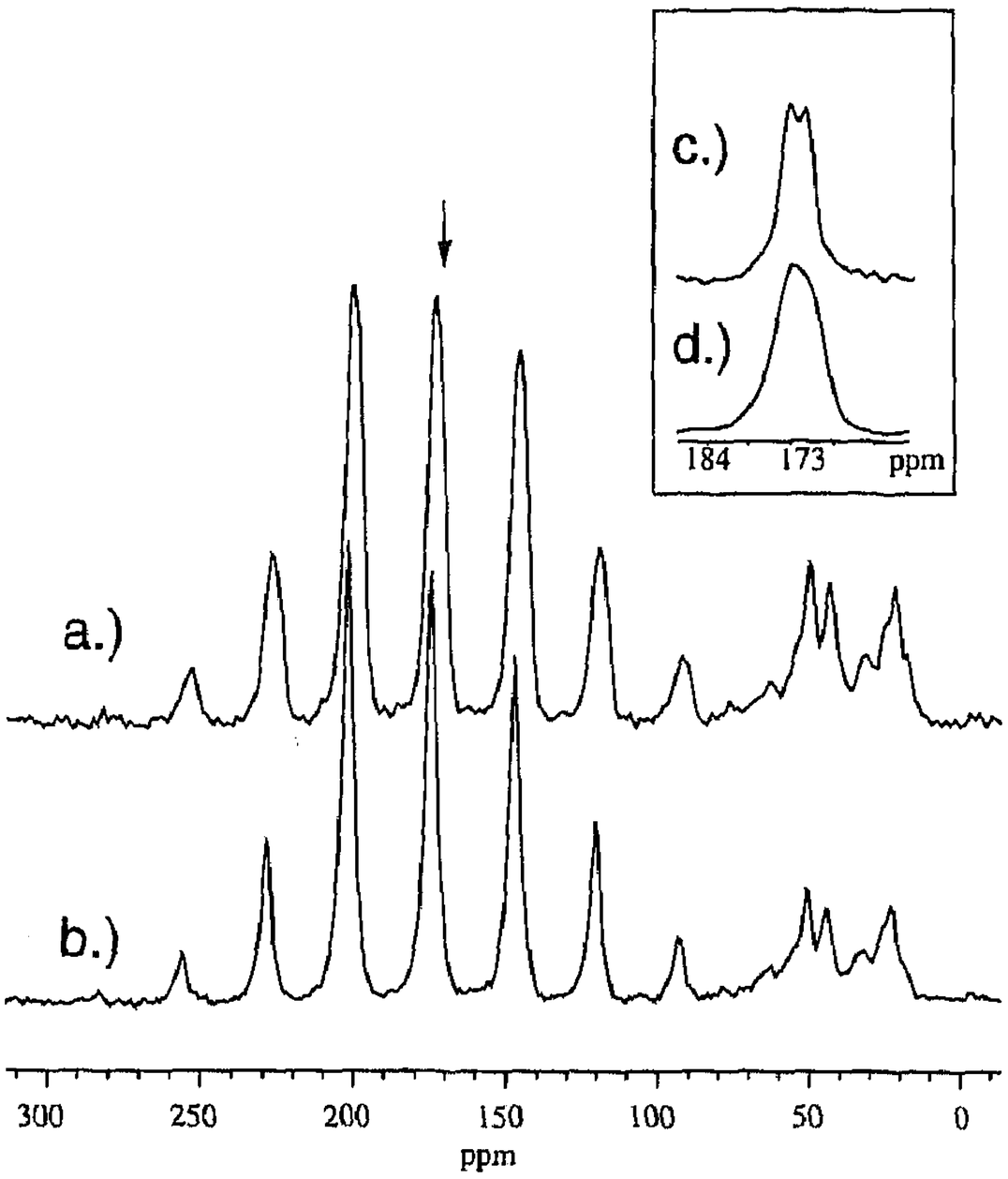

Figure 2. ^{13}C CP/MAS spectra of (a) 1-^{13}C glycine-labeled *N. madagascariensis* dragline silk and (b) 1-^{13}C alanine-labeled dragline silk. A total of 240 transients were acquired at a carbon resonance frequency of 75.47 MHz and a MAS-spinning frequency of 2 kHz. (c) Expanded centerband of the carboxylic resonances of a wet 1-^{13}C glycine-labeled spider dragline silk sample. The expanded centerband (marked with an arrow) of spectrum (a) is given in (d) for comparison.

labeling will also prove useful for the spin-diffusion experiments (vide infra). The slow-spinning ^{13}C CP/MAS spectra from the two samples are shown in Figure 2. For the alanine-labeled compound, a single resonance at $\delta_{iso} = 172.5$ ppm (FWHH = 350 Hz) is observed while the line shape of the glycine-labeled silk indicates an overlap of at least two resonances at approximately 172.5 and 169.7 ppm (see inset d of Figure 2). This indicates that glycine exists in at least two chemically distinct environments. The sideband-to-centerband intensity ratio is found, within experimental error, to be identical for the two components of the [1-^{13}C]Gly resonance, and we apply the procedure described by Herzfeld and Berger[46] to obtain the anisotropy and asymmetry of the carbon chemical shift tensors for the [1-^{13}C]Ala resonance and the total [1-^{13}C]Gly signal. The values obtained are listed in Table 1. Within experimental error, anisotropy and asymmetry are identical for [1-^{13}C]Ala and [1-^{13}C]Gly. Between 150 K and room temperature, no significant changes in the principal values were found. The line widths of the carboxylic resonances reduces upon the addition of excess water, while the isotropic chemical shifts are unaffected. For the carboxylic resonance of alanine a reduction of the line width at half-height from 350 to 240 Hz is observed upon addition of water. For the wet [1-^{13}C]glycine-labeled silk sample, two partially resolved resonances with almost equal intensities and a FWHH of 244 Hz are found (see Figure 2c), further corroborating the existence of two different environments for glycine.

Empirical relationships between the chemical shifts and the conformation of peptide chains have been found[47-49] and have indeed been used in spider silk to conclude that the alanine residues form β-sheets and that no helical structures are present in dragline silk.[34] We note that the chemical shift values of our study

Table 2. Time Constants for the ^1H-^{13}C CP Dynamics in *N. madagascariensis* Dragline Silk at Room Temperature

carbon	T_{IS} (ms)	$T_{1\rho}(^1H)$ (ms)
Gly C_α	0.28 ± 0.07	8.4 ± 1.2
Gly C=O	0.78 ± 0.09	8.2 ± 1.5
Ala C_α	0.31 ± 0.04	11.8 ± 1.7
Ala C_β	0.68 ± 0.08	12.3 ± 1.5
Ala C=O	0.50 ± 0.1	12.2 ± 3.1
Gln $C_{\beta,\gamma}$	0.29 ± 0.09	10.2 ± 1.9

coincide, within experimental error, with the values published by Simmons *et al.* if we use the glycine C=O resonance with the larger chemical shift value. In addition we have obtained information about the C=O chemical shift tensors of alanine and glycine. The alanine isotropic chemical shifts of 172.5, 48.9, and 20.5 ppm for the C=O, C_α, and C_β resonances, respectively, are clearly compatible with a β-sheet conformation. The α-helical conformation is unlikely to be a major component, while a 3_1-helical conformation, for which a model study yielded 172.1, 48.7, and 17.4 ppm,[49] could, in view of the distorted line shape of the resonance that is most dependent on the structural difference between these two forms (C_β), be a major constituent. For the glycine-rich parts of the polypeptide, structural conclusions from the chemical shifts are difficult to draw. Unfortunately, the resonance frequency of the C_α carbon of glycine does not allow a structural conclusion, in a fashion similar to that in the case of the alanine C_α resonance. Saito *et al.*[49] have noted (by comparison of the ^{13}C CP/MAS spectra of polyglycine in the form I and form II structure) that this frequency is rather insensitive to conformational changes. From the isotropic values as well as from the anisotropy and asymmetry of the chemical shift tensors of the carboxylic resonances, none of the possible conformations (α, β, 3_1, ω) at the glycine position can be excluded.[47,49]

The signal intensities in a CP-MAS spectrum must be interpreted with care because they depend not only on the relative abundance of the amino acids but also on the cross-polarization efficiency. The ^{13}C signal intensity as a function of the cross-polarization time is often characterized by an exponential buildup $I(t) \propto (1 - \exp(-t/T_{IS}))$ multiplied by a decaying exponential with a time constant $T_{1\rho}$ that describes the decay of the sum-polarization in the rotating frame.[50] The time constants T_{IS} and $T_{1\rho}$ are both rather sensitive measures for dynamical processes with correlation times in the millisecond range. For a heterogeneous sample like silk, multi-exponential buildup and decay of these line intensities may be expected. For *N. madagascariensis* dragline silk, however, the experimental results are, within experimental error, described by a single exponential for buildup and decay of each resonance. The parameters describing the CP dynamics at room temperature are compiled in Table 2 for all resolved resonances. As expected, T_{IS} is shortest for the carbons with directly bound protons. No large differences are observed for the proton $T_{1\rho}$ relaxation times of the different amino acids. These results show that the potential heterogeneity of the structure is not clearly reflected in the dynamics of the cross-polarization.

The observation of almost uniform CP dynamics with $T_{1\rho} > T_{IS}$ allows us to use the relative intensities of the individual resonances in the CP/MAS spectrum with 2 ms contact time as a rather faithful measure for the amino acid composition. Through spectral deconvolution of the aliphatic resonances in the ^{13}C CP/MAS spectrum of *N. madagascariensis* dragline silk (see

Figure 1) an estimate for the amino acid composition can be given. The relative abundance of the amino acid was found to be approximately 45%, 30%, 10%, 8%, and 4% for glycine, alanine, glutamine, serine, and tyrosine, respectively. A comparison with the amino-acid composition data of *N. clavipes* dragline silk[37] reveals no significant differences between these two members of the genus *Nephila*.

(3.2) Two-Dimensional CSA-Tensor Correlation through Spin-Diffusion. To obtain insight into the local structure in the alanine- and glycine-rich segments, two-dimensional proton-driven spin-diffusion experiments in static samples were performed. These experiments yield the relative orientation of chemical-shift tensors of nuclei in spatial proximity. "Spatial proximity" is defined such that polarization transfer between the nuclei can take place within the mixing time of the 2D experiment. In general, the spin-diffusion rate constant W_{ij} between two spins i and j depends not only on their internuclear distance r_{ij} but also on the angle θ_{ij} between the internuclear vector and the external magnetic field direction and, through the intensity of the zero-quantum spectrum at frequency zero $F_{ij}(0)$, on the chemical shift difference of the two spins i and j:

$$W_{ij} = \frac{\pi}{2}\left(\frac{\mu_0}{4\pi}\right)^2 \frac{\gamma_S{}^4 \hbar^2}{r_{ij}{}^6}\left(\frac{3\cos^2\theta_{ij} - 1}{2}\right)^2 F_{ij}(0) \qquad (1)$$

$F_{ij}(0)$ can be estimated from the experimental zero-quantum spectrum. Averaged over the chemical shift differences present in the sample, we have found a value of $F(0) \approx 5 \times 10^{-6}$ s and can therefore estimate that distances as large as 6−7 Å can be bridged by spin diffusion for a mixing time of 10 s.

As discussed in detail by Robyr *et al.*,[28] 2D spin-diffusion spectra can most easily be interpreted if the polarization transfer progresses to completion and a quasi-equilibrium state is reached where the spectrum is independent of the mixing time. In a completely ordered system, quasi-equilibrium is obtained if the slowest component of the polarization transfer establishes an equilibrium between neighboring symmetry-equivalent units. For a disordered system, quasi-equilibrium is reached if the spin diffusion has proceeded farther than the correlation length of the local order. If no quasi-equilibrium spectrum can be obtained, the interpretation of the data becomes quite involved[28] and is best done in the initial-rate regime. For our silk samples, such an analysis is not possible because signal-to-noise considerations prevented us from obtaining initial-rate spectra. It is therefore important to work in a regime where the quasi-equilibrium assumption is a reasonable one. Obviously, a heterogeneous, partially disordered material like spider silk will never allow us to obtain true quasi-equilibrium spectra. We have acquired our experimental data at a mixing time of 10 s and we adopt the assumption of quasi-equilibrium spectra for the analysis of the experimental data as a working hypothesis here. The validity of the assumption will be justified *a posteriori*.

The analysis of the quasi-equilibrium spectra yields the Euler angles between the principal axis systems of the CSA tensors of the involved nuclei. To obtain information about the relative orientation of the molecular fragments involved, the orientation in the CSA tensor in the molecular coordinate system must be known. From the study of model compounds, it has been found that, consistently, the orientation of the 1-^{13}C CSA tensor in peptides is as follows:[35,51−54] The principal axis associated with the most shielded CSA principal value δ_{33} is perpendicular to the plane spanned by the O=C—N fragment, and the principal axis associated with the intermediate component of the CSA tensor δ_{22} is almost colinear with the C=O vector. Experimental determinations of the angle between show the principal axis associated with δ_{22}, and the bond direction falls, for proteins, into the range 0−12°.

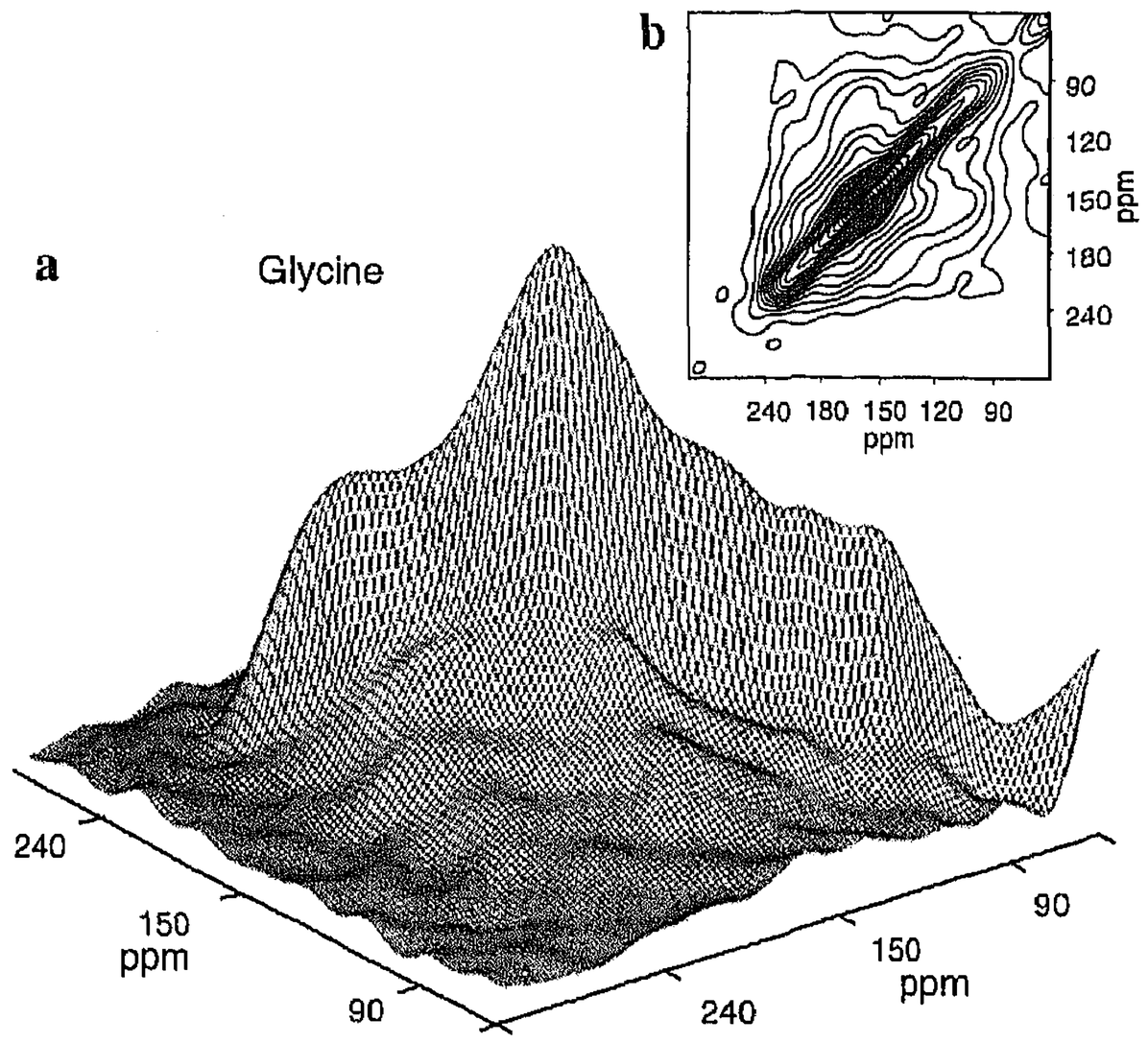

Figure 3. (a) proton-driven spin-diffusion spectrum of 1-^{13}C glycine-labeled *N. madagascariensis* dragline silk at $T = 150$ K. A mixing time of 10 s was used. The spectrum was acquired with 128 transients per data point in t_1; 96 spectra have been recorded in the F_1 domain. The data matrix of 96 × 128 points was zero-filled to 256 × 256. An exponential filter function was used prior to the double Fourier transformation. The resulting 2D spectra were symmetrized about the diagonal to enhance signal to noise. (b) Contour plot of the same data. The total signal intensity of all spectra is normalized to 1000 (for a digital resolution of 1.76 points per ppm) and equidistant contour levels are set at (±) 0.025, 0.05, 0.075, ...

The proton-driven 2D spin-diffusion spectra of [1-^{13}C]-glycine- and [1-^{13}C]alanine-labeled silk at $T = 150$ K and 10 s mixing time are given in Figures 3 and 4, respectively. The qualitative difference between the two spectra is quite striking: the spectrum of [1-^{13}C]glycine (Figure 3) shows a rather broad exchange pattern, while virtually no off-diagonal intensity is observed for the alanine carboxylic carbons (Figure 4). The degree of labeling is approximately the same for both samples. This can easily be seen from a comparison of the intensity of the labeled C=O resonances with the natural abundance signals in Figure 2a,b.

The absence of cross-peaks in alanine indicates that either the spin diffusion between alanines is very slow because they are well separated in space or the poly-alanine regions are highly ordered with all three principal axes of carboxylic CSA tensors being either parallel or antiparallel. The zero-quantum line shape can be assumed to be of the same order of magnitude for both amino acids.[17] If we assume that the primary structure of *N. madagascariensis* silk is similar to that of *N. clavipes*, then the first explanation is highly improbable because its primary structure[37,38] consists of alanine rich segments. We conclude therefore that close-by [1-^{13}C]alanine CSA tensors have approximately colinear principal axis systems.

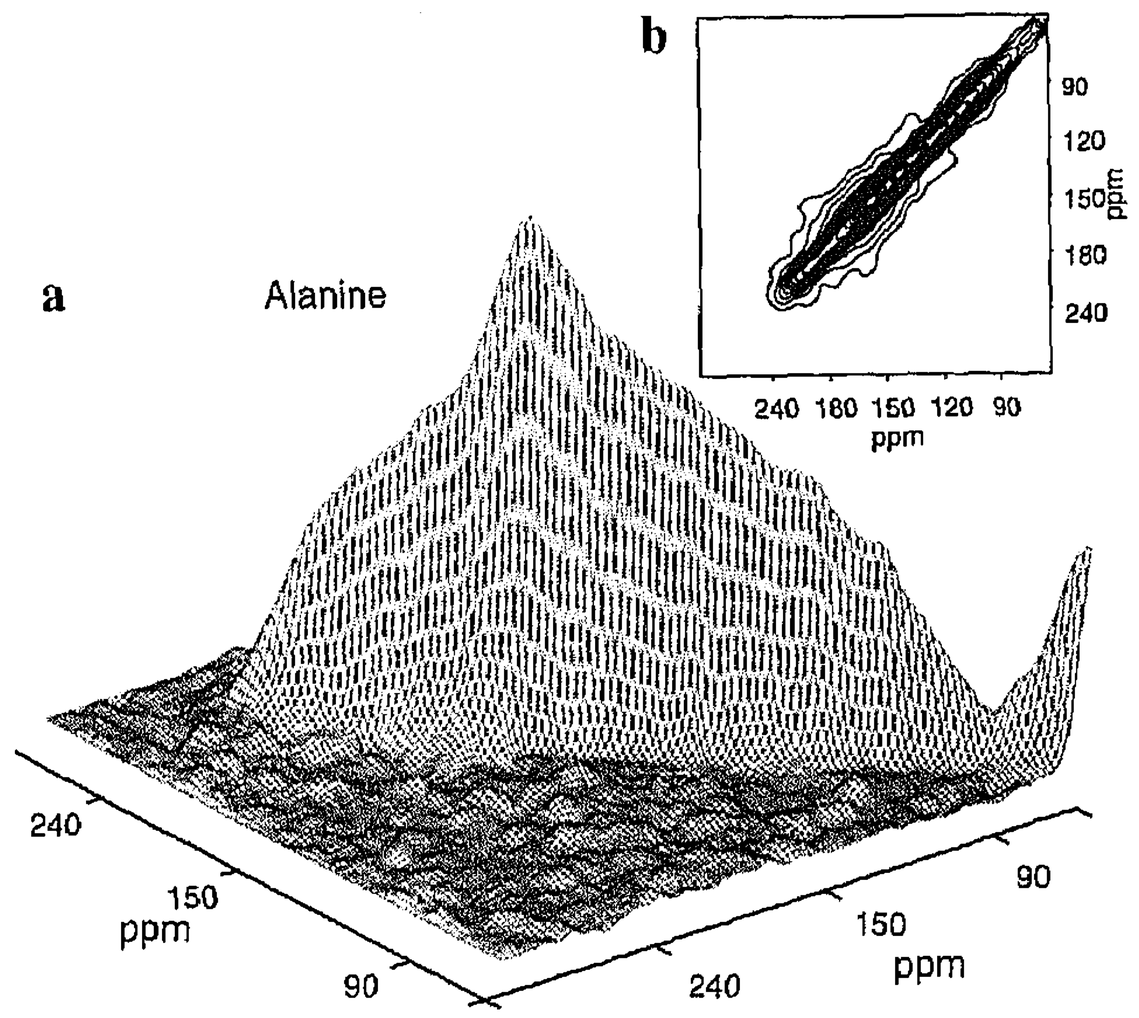

Figure 4. (a) Proton-driven spin-diffusion spectrum of 1-^{13}C alanine-labeled *N. madagascariensis* dragline silk taken under conditions identical to the spectrum of Figure 3. (b) Contour plot of the same data. Contour levels are chosen as described in the caption of Figure 3.

A structure where most alanines are incorporated into an ordered β-sheet structure explains these experimental findings. Taking into account the experimental line shape, we find that the spectrum of Figure 4 confines all three Euler angles to be 0 ± 10 or $180 \pm 10°$.

The spectrum from the glycine-labeled samples exhibits a nonisotropic exchange pattern with a two-dimensional line shape strongly deviating from the 2D product of the one-dimensional line shape function[28] given in Figure 5a. Therefore, the local packing must be ordered.[28] Because not much is known about the interchain packing and the resulting interchain distances, we shall consider models with both intra- and interchain interactions to explain the experimental spectra.

Let us first consider intrachain spin diffusion only. We assume that the spin diffusion has equalized the polarization over many (>10) carbon atoms within one chain. This is a reasonable assumption because the rate constant obtained from eq 1 is much faster than the inverse mixing time. This is true not only for ^{13}C in amino acids adjacent in the primary sequence (where an average rate constant of about 5 s^{-1} is predicted) but also for ^{13}C in amino acids separated by two in the primary sequence. A random coil arrangement would then lead to a spectrum closely resembling the amorphous spectrum of Figure 5a and can be excluded. β-sheet structures can also be excluded because they would lead again to an almost diagonal 2D spectrum. We shall, in the following, test the compatibility of two other plausible structures, the α-helix and 3_1-helix with the experimental data of Figure 3.

For an α-helical structure (see Figure 6) all C=O bond directions are approximately parallel to the helical chain axis. Correspondingly, the principal axis directions associated with the Cartesian σ_{yy} components of all ^{13}C CSA tensors coincide approximately with the helix axis. The relative tensor orientation between two neighboring carboxylic CSA tensors is therefore described by a rotation around the y axis of the principal axis system of the CSA tensor, corresponding to a set of Euler angles (0°, 100°, 0°). From a simulated poly(Gly−Gly−X) α-helix (with X = Ala), obtained with the program

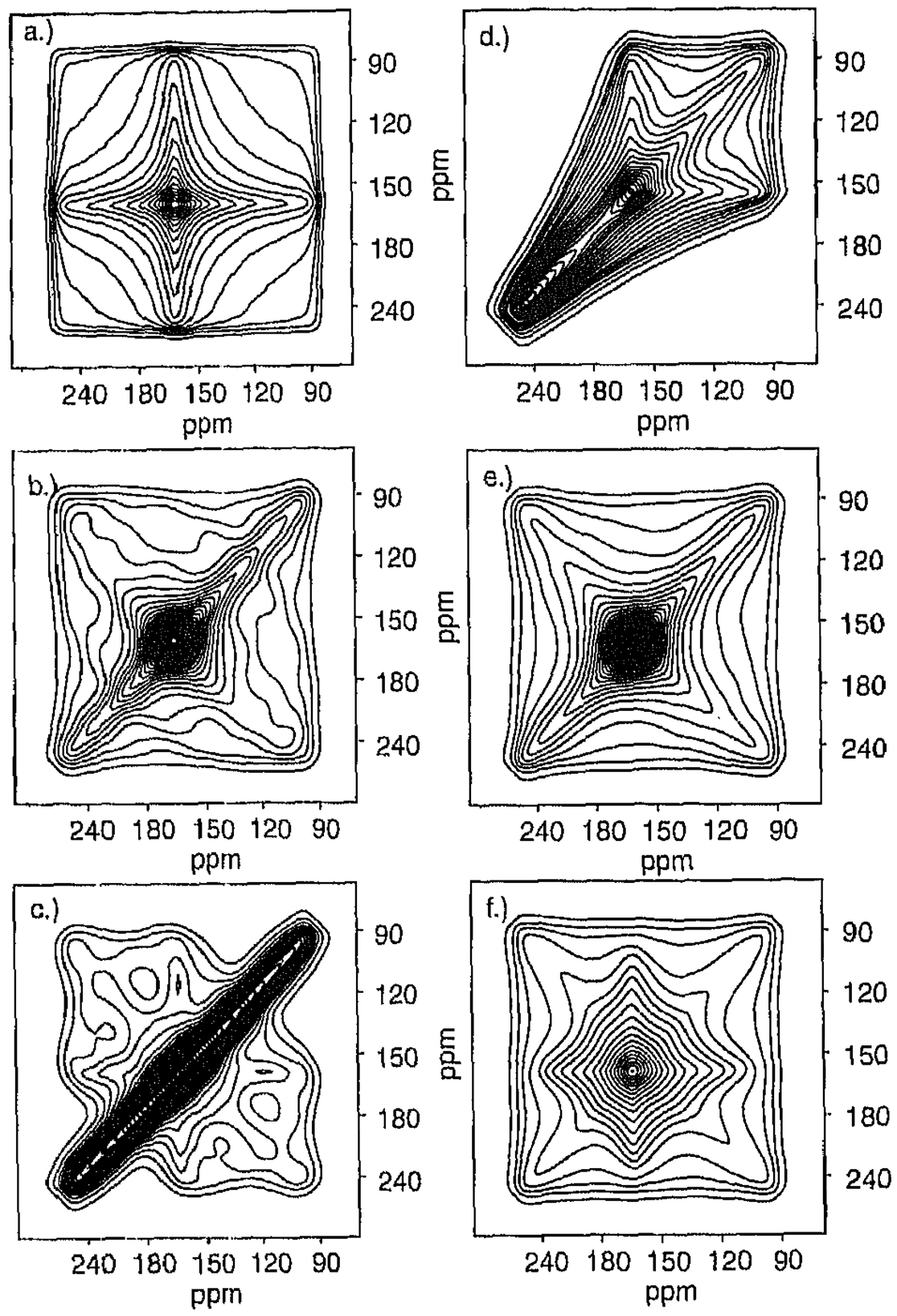

Figure 5. Simulations of 2D spin-diffusion powder spectra at quasi-equilibrium for the ^{13}C=O resonance in glycine. The following structures were assumed: (a) amorphous spectrum; (b) isolated α-helix (or fully ordered array thereof); (c) 3_1-helix using Euler angles between the CSA principal axis systems of $\alpha = 114°$, $\beta = 78°$, and $\gamma = 346°$ (see text); (d) uniaxially ordered array of 2_1-helices, taking into account 50 nuclei and assuming that the helix axis coincides with the principal axis belonging to δ_{11}; (e) uniaxially ordered array of α-helices, taking into account 50 nuclei and assuming that the helix is parallel to δ_{22}; (f) uniaxially ordered array of 3_1-helices, taking into account 50 nuclei and using the Euler angles given in the text. The simulations were performed in the frequency domain using the simulation environment GAMMA and following the general scheme of the example given in ref 60. For the simulations the same resolution (1.76 points/ppm) as in the experimental spectra was chosen.

Quanta,[55] Euler angles of (65.4°, 97.7°, 189.9°) = (−14.6°, 97.7°, 9.9) are extracted. The quasi-equilibrium spectrum of an isolated (Gly−Gly−X)$_n$ α-helical structure, where 3.6 residues constitute one turn and the helix is repeated after five turns, is described by a polarization exchange between 12 glycine sites (the X residues are not ^{13}C labeled). Figure 5b shows the simulated quasi-equilibrium spectra for spin diffusion between all ^{13}C in an isolated helix. The spectrum clearly disagrees with the experimental data of Figure 3.

Next we consider a 3_1-helical arrangement (see Figure 6). Such a structure is found, for example, for the form II crystal structures of poly-Gly,[56,57] poly(L-Ala−Gly−Gly),[58] poly(L-Ala−Gly−Gly−Gly),[58] and poly(Gly-β-Ala).[59] In a (Gly−Gly−X)$_m$-3_1-helical structure only two symmetrically inequivalent [1-^{13}C]Gly sites exist and the quasi-equilibrium spectrum corresponds to a two-site exchange spectrum.

From a model (Gly−Gly−Ala)$_n$ polypeptide produced by the program Quanta[55] the Euler angles that relate

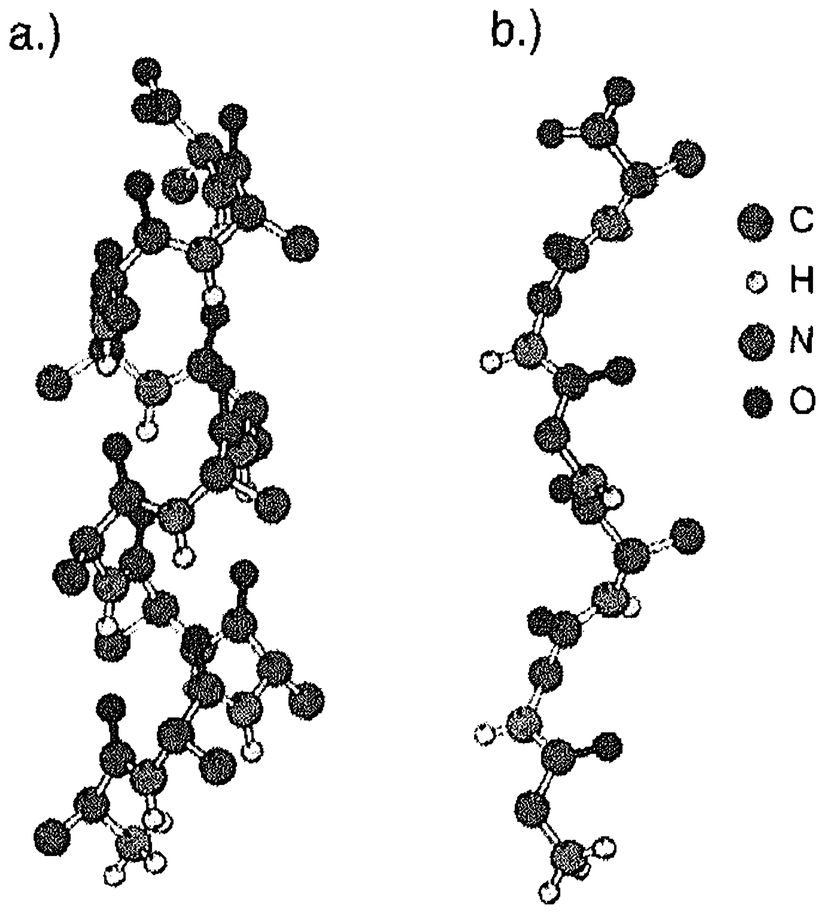

Figure 6. (a) Conformation of an α-helix. (b) Conformation of a 3_1-helix. The C=O bond direction (indicated by filled bond symbols) is approximately along the helical axis direction in the α-helix and almost perpendicular to it in the 3_1-helix. In contrast to the α-helical structures which are stabilized by intrachain hydrogen bonds, 3_1-helices are stabilized by interchain hydrogen bonds. The figures were created with the program MOLSCRIPT.[67]

the O=C—N fragments of each glycine residue were found to be $\alpha = 114°$, $\beta = 78°$, and $\gamma = 346°$. A simulated quasi-equilibrium 2D spin-diffusion spectrum assuming spin exchange between glycine sites related by these Euler angles is depicted in Figure 5c. For all simulations, the GAMMA programming environment was used.[60] The total signal intensity of all spectra presented in this paper is normalized by the same procedure described in the legend of Figure 3. Therefore the contour levels in all figures can directly be compared. Qualitatively, the simulated spectrum resembles the experimental spectrum of Figure 3.

To improve the description of the experimental spectrum, we fit the data in Figure 3 by a quasi-equilibrium spin-diffusion spectrum between *two* magnetically nonequivalent sites. Starting from the spectrum in Figure 5c the Euler angles are optimized by means of a nonlinear least mean squares fit.[61] Free parameters of the fit are the set of Euler angles (α, β, γ) and the line width. We assume the line shape to be Lorentzian with a constant full width at half-height over the 2D spectrum. Furthermore, we allowed for a superposed signal with an isotropic powder exchange spectrum to account for spin diffusion between chains. The fraction of the isotropic exchange spectrum yields a fifth parameter for the fit. The chemical shift parameters were set to the values determined from the 1D spectra. The best fit, shown in Figure 7b, reproduces the off-diagonal features of the experimental 2D spin-diffusion spectrum (Figure 7a) remarkably well. The fitted Euler angles are $\alpha = 101 \pm 13°$, $\beta = 62 \pm 14°$, and $\gamma = 333 \pm 10°$ (error estimated at 90% confidential limit) and an admixture of $14 \pm 5\%$ signal intensity from an isotropic exchange pattern. The absolute value of the difference between the experimental spectrum and the best fit amounts to 12% of the integrated intensity of the experimental spectrum. If we do not allow for an isotropic powder pattern as part of the model, the difference between the calculated and experimental spectrum rises to 23%. The difference spectrum is depicted in Figure 7c and gives no indication that the quasi-equilibrium spectrum is distorted through the influence of the factor $F_{ij}(0)$ which would lead to a monotonic decrease of the cross-peak

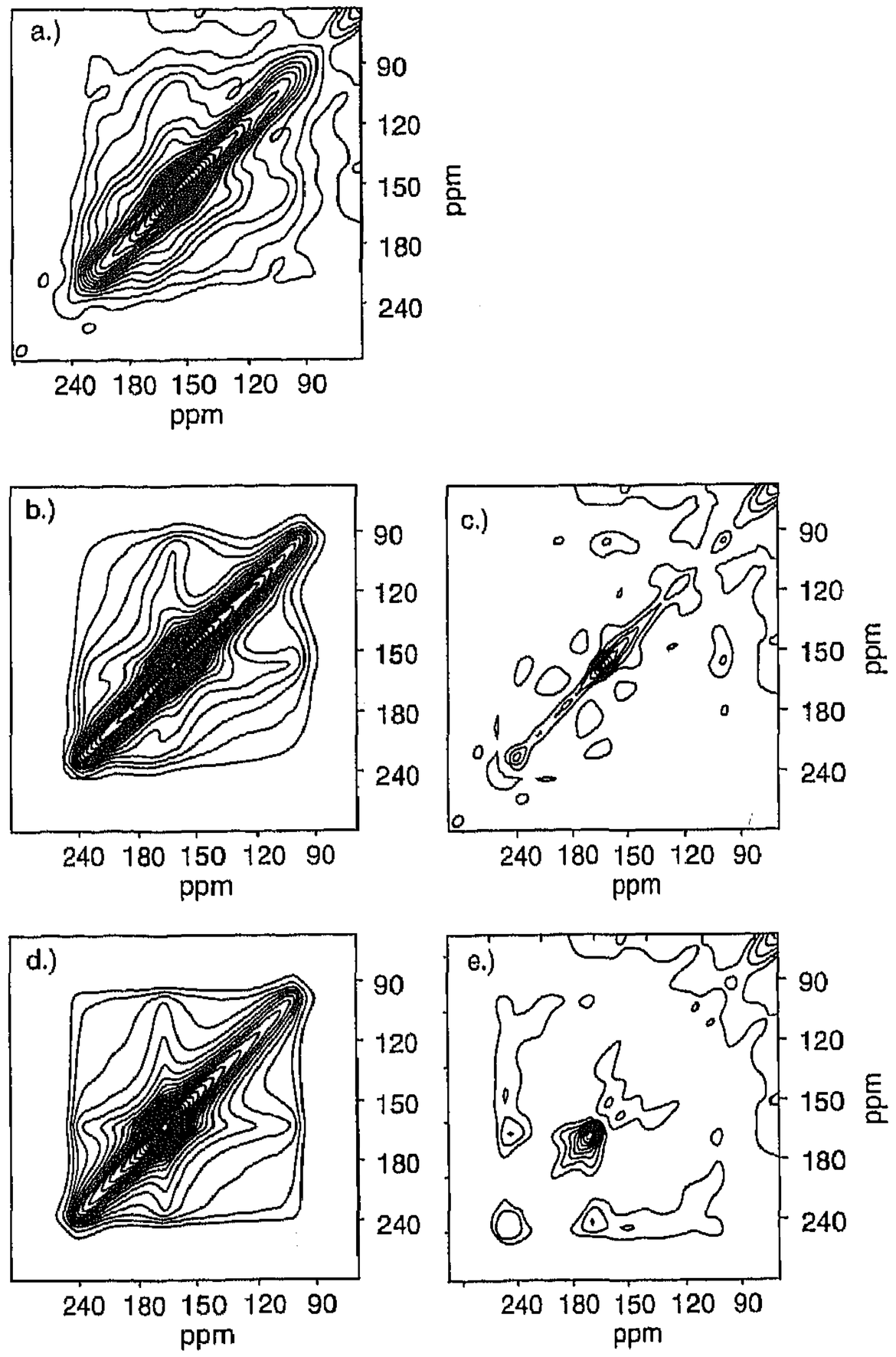

Figure 7. (a) Experimental spectrum 1-^{13}C glycine (see also Figure 3), replotted for direct comparison with (b)—(e). (b) Best fit of the experimental spectrum by a two-site exchange model with an amorphous background, as described in the text. The conformation represents, within reasonable expectations (see text), a 3_1-helical structure. (c) Difference between the experimental spectrum (a) and fit (b). (d) Best fit by a superposition of an amorphous and a diagonal spectrum (see text). (e) Difference between (a) and (d). Contour levels are chosen as described in the legend of Figure 3.

intensity with increasing distance from the main diagonal of the spectrum. The main difference intensity appears along the diagonal itself, particularly at the sharp features of the tensor. The pronounced intensity at the sharp features indicates non-Lorentzian line shapes and the remaining intensity over the entire diagonal implies that complete polarization transfer between all glycines in the sample has not been established. The remaining diagonal signal may be attributed to glycines that are located outside the (Gly—Gly—X) segments[37] and therefore more remote from the next Gly neighbor. This, as well as the relatively small intensity of the diagonal ridge and the absence of a decay of the experimental cross-peak intensity (compared to the simulation) perpendicular to the diagonal of the spectrum, is a good *a posteriori* justification of the assumption of quasi-equilibrium conditions. We have repeated the fit with starting values that correspond to an α-helical conformation and have found that it converges to the same 3_1-helical structure described above.

The fitted Euler angles deviate by about 15° from the idealized $(Gly—Gly—X)_n$ structure. These deviations can be explained by structural distortions and/or the deviation of the principal-axis directions of the CSA tensor

from the idealized values. Therefore, the spin-diffusion data are in good agreement with a 3_1-helical structure formed by the (Gly–Gly–X)$_n$ segments of the protein.

The overall agreement between the certainly oversimplified model and the experimental spectrum may, considering the heterogeneous nature of the dragline silk as well as the possible experimental imperfections, be fortuitously good. We shall now shortly investigate possible other models that explain the experimental spectrum but assume significant interchain spin diffusion. Obviously, the random-chain model spectra of Figure 5a is not changed by taking into account interchain diffusion. All the other model spectra also approach the spectrum of Figure 5a if interchain diffusion between completely disordered chains ("spaghetti model") is assumed. Because this prediction is in contradiction with the experiment, we consider next uniaxially ordered bundles of chains. For such a model bundle, quasi-equilibrium spectra for 2_1-helices, α-helices, and 3_1-helices, respectively, are shown in Figure 5a–f. No satisfactory agreement with the experimental data is found.

As a further step, we may consider more complex models which describe heterogeneous situations. We therefore consider an amorphous spectrum (from a random-coil domain) superposed with a diagonal spectrum from isolated glycines. Using the line width and the relative amount of diagonal spectrum as free parameters, a least squares fit to the experimental spectrum was performed. The best fit yields 31 ± 4% isolated glycine, the resulting spectrum is shown in Figure 7d, and the difference between experiment and fit is given in Figure 7e. The agreement is not satisfactory and leaves 25% of the spectral intensity unexplained. Furthermore, we have observed that the carboxylic signal of a uniaxially oriented bundle of fibers shows a significant deviation from the powder pattern obtained from an unoriented sample.[62] On the basis of these two arguments, we exclude amorphous random coils as a *major* component of the structure. A large number of further heterogeneous structures could be considered. We shall refrain, in the present context, from doing so because the simple 3_1-helical model shows already a good agreement with the experiment.

It should be pointed out that the off-diagonal peaks in the spectrum of Figure 3 could also be caused by chemical exchange instead of spin exchange or by the simultaneous action of both processes. Usually, the temperature dependence of the cross-peak intensity allows for a distinction of the two effects: the spin diffusion is largely temperature independent while an Arrhenius-type activation is expected for the chemical exchange. While the full information available by spin-diffusion spectroscopy is contained only in two-dimensional static spectra, selective 1D experiments under magic-angle spinning conditions can be used to extract partial information using shorter total measurement times,[27] although a direct comparison between spin-diffusion rate constants in static and rotating samples is difficult. The one-dimensional analog of the exchange experiment proposed by Yang et al.[43] was chosen to follow the polarization-transfer process as a function of temperature and to extend the spin diffusion measurements to longer mixing times. The one-dimensional spectrum obtained in this experiment does not contain the entire spinning-sideband manifold but only the centerband if no exchange (spin diffusion or chemical exchange) takes place in the mixing time of the experiment. If, however, one of the processes is active, the special magnetization state prepared by the TOSS sequence[27,63–65] is disturbed and spinning sidebands are reintroduced into the spectrum. A series of spectra recorded with different mixing times allows us therefore to extract information similar to that from the 2D spin-diffusion spectrum with the difference that only a limited number of sampling points are available. Figure 8 plots the TOSS centerband and sideband intensities in ^{13}C spectra of the [1-^{13}C]glycine-labeled sample obtained with the 1D experiment as a function of mixing time; the sample temperature was 220 K. It can easily be seen that on an increase of the mixing time the intensity of the centerband decreases exponentially (with a time constant of 6.3 ± 0.5 s) and spinning sideband intensity is reintroduced monotonically. For the long mixing times used in the experiments magnetization losses due to T_1 relaxation are considerable and the total intensities of the spectra at different mixing times have been normalized in Figure 8. These data are a further indication that the assumption of an established quasi-equilibrium after 10 s of mixing, used for the interpretation of the 2D spectra, is a reasonable one.

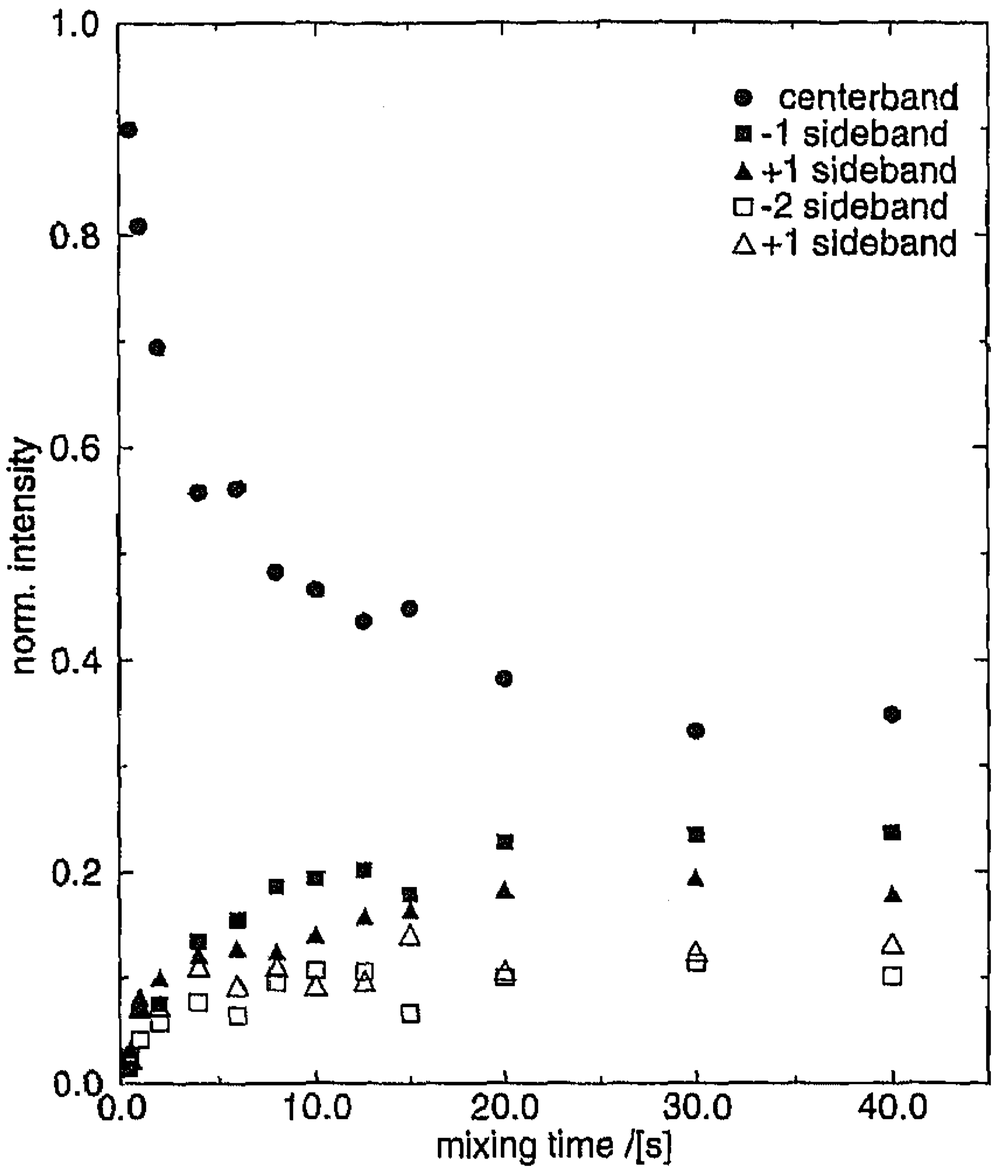

Figure 8. Mixing-time dependence of the centerband and spinning sideband intensities in the TOSS-exchange experiment on 1-^{13}C glycine-labeled dragline silk at $T = 220$ K. The spectra were acquired at 125.8 MHz carbon frequency with a magic-angle spinning frequency of 3.5 kHz.

Figure 9 depicts the resulting 1D TOSS spectra of the [1-^{13}C]glycine-labeled sample using a mixing time of 10 s for temperatures of 220 and 293 K. The temperature dependence of the spectra and, therefore, of the spin-diffusion rate constant is negligible and leads us to the conclusion that contributions from chemical exchange to the spectrum of Figure 3 (recorded at an even lower temperature) can be excluded.

(4) Conclusions

We have shown that the secondary structures of the alanine-rich and glycine-rich segments of spider dragline silk can be characterized by means of proton-driven ^{13}C 2D spin-diffusion experiments. Our results are in good agreement with the following structural model for *N. madagascariensis* dragline: The polyalanine seg-

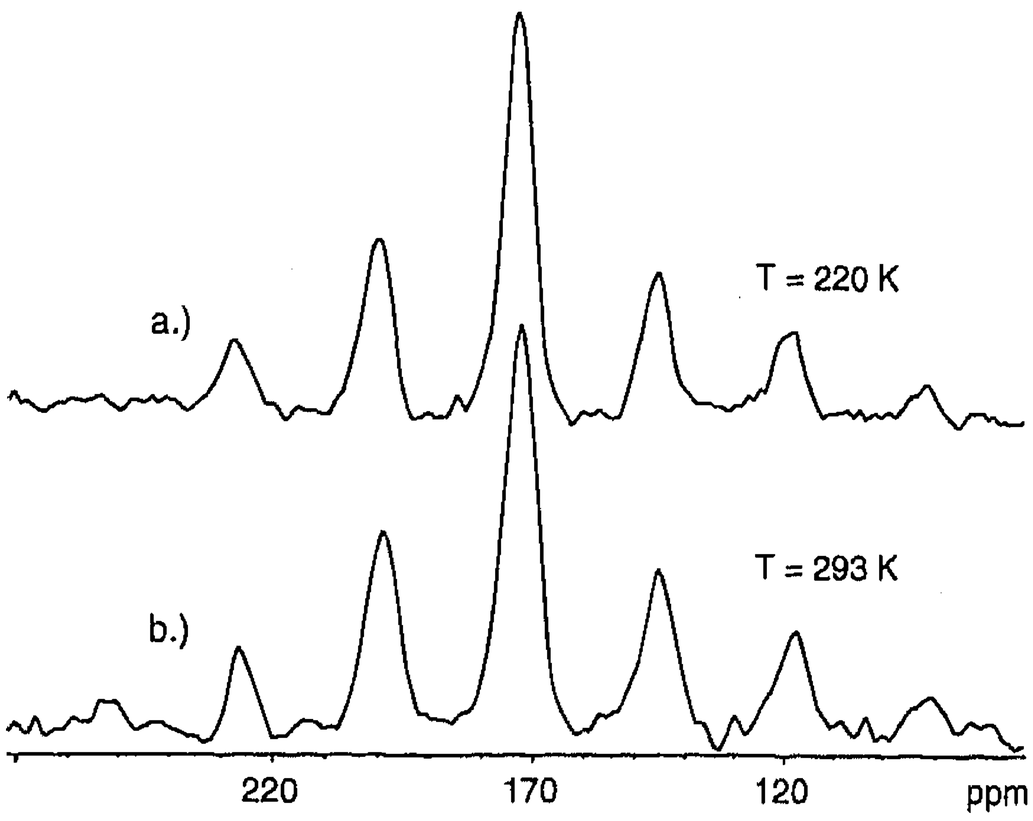

Figure 9. TOSS-exchange spectra of 1-^{13}C glycine-labeled dragline silk (125.8 MHz resonance frequency) at sample temperatures of (a) $T = 220$ K and (b) $T = 293$ K. The mixing time was set to 10 s, the spinning frequency, to 3.5 kHz, 32 transients were coadded.

ments adopt a highly ordered β-sheet structure whereas the glycine-rich segments form 3_1-helical structures. Considering the relatively short length of these segments and the resulting constraints on the packing scheme of the solid, these idealized structures are astonishingly well represented in the experimental spectra. Obviously, there may be more complicated structural models for the glycine-rich domains that can also explain the experimental data. β-Sheets and α-helices can, however, be excluded on the basis of our data.

It is obvious that an explanation of the mechanical properties of spider dragline does not only demand the knowledge of the secondary structure of the different domains in the protein. The local packing, i.e. the domain size of the β-sheet structures and the packing of the 3_1-helices, is required for a complete understanding of the macroscopic properties. Nevertheless, one might speculate that the extremely strong mechanical properties of silk may be related to the presence of 3_1-helical structures because they are able to form interhelix hydrogen bonds cross-linking the helices. A detailed analysis of the packing schemes of the helices among themselves requires multiple labeled samples and experiments with macroscopically aligned fiber samples. Work along these lines is in progress in our laboratory.

Acknowledgment. We thank Prof. Dr. R. R. Ernst (ETH Zürich, Switzerland) and PD. Dr. A. Sebald (Bayerisches Geo-Institut, University of Bayreuth, Germany) for their generosity. The SON National HF-NMR Facility, University of Nijmegen, and the Danish SNF gave generous support. We thank H. B. Jørgensen for silking the spiders. J.K. acknowledges financial support by the Ciba-Geigy Jubiläums-Stiftung and by the Deutsche Forschungsgeneinschaft.

References and Notes

(1) Work, R. W. *Text. Res. J.* **1977**, *47*, 650–662.
(2) Denny, M. W. Silks—their properties and functions. In *The mechanical properties of biological materials*; Vincent, J. F. V., Currey, J. D., Eds.; Society for Experimental Biology, Symposia; Cambridge University Press: Cambridge, U.K., 1980; Vol. 34, pp 245–271.
(3) Gosline, J. M.; DeMonte, M. E. D.; Denney, M. W. *Endeavor* **1986**, *10*, 37–43.
(4) Cunnif, P. M.; Staufer, S. L.; Lewis, R. V. In *Silk Polymers—Materials Science and Biotechnology*; Kaplan, D., Adams, W. W., Farmer, B., Viney, C., Eds.; American Chemical Society: Washington, DC, 1994; p 222.
(5) Kovoor, J. Comparative Structure and Histochemistry of silk-producing organs in Arachnids. In *Ecophysiology of Spiders*; Nentwig, W., Ed.; Springer: Berling, Heidelberg, New York, 1987; pp 160–186.
(6) Vollrath, F. *Sci. Am.* **1992**, *266*, 70–76.
(7) Magoshi, J.; Magoshi, Y.; Nakamura, S. *J. Appl. Polym. Sci.* **1985**, *41*, 187–201.
(8) Kerkam, K.; Viney, C.; Kaplan, D.; Lombardi, S. *Nature* **1991**, *349*, 596–598.
(9) Work, R. W. *J. Arachnol.* **1981**, *9*, 299–308.
(10) Kaplan, D. L.; Adams, W. W.; Viney, C.; Farmer, B. L. In *Silk Polymers—Materials Science and Biotechnology*; Kaplan, D., Adams, W. W., Farmer, B., Viney, C., Ed.; American Chemical Society: Washington, DC, 1994.
(11) Gosline, J.; Denny, M.; deMont, M. *Nature* **1984**, *309*, 551–552.
(12) Gosline, J. M.; Pollak, C. C.; Agurette, P.; Cheng, A.; DeMont, M. E.; Denny, M. W. Elastomeric Network Models for the Frame and Viscid Silks from the Orb Web of the Spider *Araneus diadematus*. In *Silk Polymers—Materials Science and Biotechnology*; Kaplan, D., Adams, W. W., Farmer, B., Viney, C., Eds.; American Chemical Society: Washington, DC, 1994; pp 328–341.
(13) Work, R. W. *J. Exp. Biol.* **1985**, *118*, 379.
(14) Mitchell, G. R. In *Comprehensive Polymer Science*; Pergamon: Oxford, U.K., 1989; Vol. 1, Chapter 31.
(15) Griffiths, J. M.; Griffin, R. B. *Anal. Chim. Acta* **1993**, *283*, 1081.
(16) Bennet, A. E.; Griffin, R. G.; Vega, S. *Recoupling of Homo- and Heteronuclear Dipolar Interactions in Rotating Solids*; NMR Basic principles and progress, Solid-State NMR IV; Springer Verlag: Berlin, Heidelberg, 1994; Vol. 33.
(17) Meier, B. H. Polarization Transfer and Spin Diffusion in Solid-State NMR. In *Advances in Magnetic and Optical Resonance*; Warren, W. S., Ed.; Academic Press: New York, 1994; Vol. 18, pp 1–116.
(18) Bloembergen, N. *Physica* **1949**, *15*, 386.
(19) Assink, R. A. *Macromolecules* **1978**, *11*, 1233.
(20) Caravatti, P.; Deli, J. A.; Bodenhausen, G.; Ernst, R. R. *J. Am. Chem. Soc.* **1982**, *104*, 5506.
(21) Caravatti, P.; Neuenschwander, P.; Ernst, R. R. *Macromolecules* **1985**, *18*, 119.
(22) Tycko, R.; Dabbagh, G. *J. Am. Chem. Soc.* **1991**, *113*, 5392.
(23) Tycko, R.; Dabbagh, G. *Mater. Res. Soc. Symp. Proc.* **1991**, *215*, 125.
(24) Dabbagh, G.; Weliky, D. P.; Tycko, R. *Macromolecules* **1994**, *27*, 6183.
(25) Robyr, P.; Meier, B. H.; Ernst, R. R. *Chem. Phys. Lett.* **1991**, *187*, 471.
(26) Robyr, P.; Meier, B. H.; Fischer, P.; Ernst, R. R. *J. Am. Chem. Soc.* **1994**, *116*, 5315–5323.
(27) Schmidt-Rohr, K.; Spiess, H. W. *Multidimensional Solid-State NMR and Polymers*; Academic Press: London, 1994.
(28) Robyr, P.; Tomaselli, M.; Straka, J.; Grob-Pisano, C.; Suter, U. W.; Meier, B. H.; Ernst, R. R. *Mol. Phys.* **1995**, *84*, 995–1020.
(29) Ernst, R. R.; Bodenhausen, G.; Wokaun, A. *Principles of Nuclear Magnetic Resonance in One and Two Dimensions*; Clarendon Press: Oxford, U.K., 1987.
(30) Jeener, J.; Meier, B. H.; Bachmann, P.; Ernst, R. R. *J. Chem. Phys.* **1979**, *71*, 4546.
(31) Edzes, H. T.; Bernards, J. P. C. *J. Am. Chem. Soc.* **1984**, *106*, 1515.
(32) Henrich, P. M.; Linder, M. *J. Magn. Reson.* **1984**, *58*, 458.
(33) Robyr, P.; Meier, B. H.; Ernst, R. R. *Chem. Phys. Lett.* **1989**, *162*, 417.
(34) Simons, A.; Ray, E.; Jelinski, L. W. *Macromolecules* **1994**, *27*, 5235–5237.
(35) Saito, H. *Magn. Reson. Chem.* **1986**, *24*, 835–852.
(36) Candelas, G.; Candelas, T.; Ortiz, A.; Rodriguez, O. *Biochem. Biophys. Res. Commun.* **1983**, *116*, 1033–8.
(37) Mello, C. M.; Senecal, K.; Yeung, B.; Voudros, P.; Kaplan, D. In *Silk Polymers—Materials Science and Biotechnology*; Kaplan, D., Adams, W. W., Farmer, B., Viney, C., Eds.; American Chemical Society: Washington, DC, 1994; p 67.
(38) Lewis, R. V. *Acc. Chem. Res.* **1992**, *25*, 392–398.
(39) Warwicker, J. O. *J. Mol. Biol.* **1960**, *2*, 350–362.
(40) Thiel, B. L.; Kunkel, D. D.; Viney, C. *Biopolymers* **1994**, *34*, 1089–1097.
(41) Dong, Z.; Lewis, R. V.; Middaugh, C. R. *Arch. Biochem. Biophys.* **1991**, *284*, 53–57.

(42) Work, R. W.; Emerson, P. D. *J. Arachnol.* **1982**, *10*, 1–10.
(43) Yang, Y.; Schuster, M.; Blümich, B.; Spiess, W. H. *Chem. Phys. Lett.* **1987**, *139*, 239.
(44) deJong, A.; Kentgens, A. P. M.; Veeman, W. S. *Chem. Phys. lett.* **1984**, *109*, 337.
(45) Kümmerlen, J.; Sebald, A.; Weigel, R. *Solid State Nucl. Magn. Reson.* **1992**, *1*, 231.
(46) Herzfeld, J.; Berger, A. *J. Chem. Phys.* **1980**, *73*, 6021.
(47) Ando, S.; Yamanobe, T.; Ando, I.; Shoji, A.; Ozaki, T.; Tabeta, R.; Saito, H. *J. Am. Chem. Soc.* **1985**, *107*, 7648–7652.
(48) Saito, H.; Iwanga, Y.; Tabeta, R.; Narita, M.; Asakura, T. *Chem. Lett.* **1983**, 427.
(49) Saito, H.; Tabeta, R.; Shoji, A.; Oazki, T.; Ando, I.; Miyata, T. *Biopolymers* **1984**, *23*, 2279–2297.
(50) Mehring, M. *Principles of High Resolution NMR in Solids*, 2nd ed.; Springer: Berlin, 1983.
(51) Hartzell, C. J.; Pratum, T. K.; Drobny, G. *J. Chem. Phys.* **1987**, *87*, 4324–31.
(52) Separovic, F.; Smith, R.; Yannoni, C. S.; Cornell, B. A. *J. Am. Chem. Soc.* **1990**, *112*, 8324–8.
(53) Teng, Q.; Iqbal, M.; Cross, T. A. *J. Am. Chem. Soc.* **1992**, *114*, 5312–21.
(54) Stark, R. E.; Jelinski, L. W.; Ruben, D. J.; Torchia, D. A.; Griffin, R. G. *J. Magn. Reson.* **1983**, *55*, 266–73.
(55) Quanta4.0 is a commercial Program from Molecular Simulations Inc., Burlington, MA.
(56) Crick, F. H. C.; Rich, A. *Nature* **1955**, *176*, 780.
(57) Ramachandran, G. N.; Sasisekharan, V.; Ramakrishnan, C. *Biochem. Biophys. Acta* **1966**, *112*, 168–170.
(58) Lotz, B.; Keith, H. D. *J. Mol. Biol.* **1971**, *61*, 195.
(59) MunozGuerra, S.; Fita, I.; Aymami, J.; Puiggali, J. *Macromolecules* **1988**, *21*, 3464.
(60) Smith, S.; Levante, T.; Meier, B. H.; Ernst, R. R. *J. Magn. Reson. A* **1994**, *106*, 75–105.
(61) Program MINUIT was used. This is part of the PACKLIB program package. It was obtained under the conditions of the CERN Program Library/Division CN, CERN 1211 Geneva, Switzerland.
(62) Kümmerlen, J.; van Beek, J.; Vollrath, F.; Meier, B. H. Manuscript in preparation.
(63) Dixon, W. T. *J. Chem. Phys.* **1982**, *77*, 1800.
(64) Dixon, W. T.; Schaefer, J.; Sefcik, M. D.; Stejskal, E. O.; McKay, R. A. *J. Magn. Reson.* **1982**, *49*, 341.
(65) Raleigh, D. P.; Olejniczak, E. T.; Vega, S.; Griffin, R. G. *J. Magn. Reson.* **1987**, *72*, 238.
(66) Haeberlen, U. *High Resolution NMR in Solids: Selective Averaging*; Academic Press: New York, 1968.
(67) Kraulis, P. J. *J. Appl. Crystallogr.* **1991**, *24*, 945–9.

MA951098I